

# Research Journal of Pharmaceutical, Biological and Chemical Sciences

## Direct Current Electrical Conductivity Study of the Thermal Decomposition of Copper (II) Monohydrate and Zinc (II) Oxalate Dihydrate.

Athare AE<sup>1\*</sup>, Nikumbh AK<sup>2</sup>, and Kolhe NH<sup>1</sup>

<sup>1</sup> New Arts Commerce and Science College Ahmednagar-414001, India

<sup>2</sup> Department of Chemistry, University of Pune, Ganeshkhind, Pune 411007, India

### ABSTRACT

The solid state reactions involved in the preparation of copper oxide and zinc oxide from copper(II) and Zinc (II) oxalate of monohydrated and dihydrate respectively have been analyzed using direct current electrical conductivity measurement under the atmospheres of static air, dynamic dry nitrogen and dynamic air. The product at each decomposition stage have been characterized by infrared spectroscopy and X-ray powder diffraction. For Copper (II) oxalate monohydrated the final decomposition product in all three atmospheres was found to be CuO and intermediate step product was Cu<sub>2</sub>O. The Zinc (II) oxalate dehydrated also shows final product in all three atmospheres was found to be ZnO. The conductivity measurement were supplemented with data obtained by chemical thermal (TGA and DTA), IR spectroscopy and X-ray powder diffraction analysis.

**Keywords:** Thermal decomposition, Cu, Zn-Oxalates, d.c. electrical conductivity.

*\*Corresponding author*

Email: Itanilathare@gmail.com

## INTRODUCTION

Thermal analysis-thermogravimetry(TGA),differential thermogravimetry(DTG) and differential thermoanalysis (DTA) are widespread and helpful instruments in the hand of the chemist to reveal the energies of phase transition and chemical reaction ,the thermal stabilities of educts and products as well as the nature and consistency of gaseous reaction products .of itself thermal analysis provides only weak clues pertaining to reaction mechanisms , especially to the broadness of DTG and DTA peak ,the various intermediates formed during this step could not be detected; further the TGA curve exhibited continuous weight loss until crystallization to metal oxide occurred . This is the principal shortcoming of the method but can be overcome by use of direct current electrical conductivity, which allow the formation of intermediates of varying conductivity.

The thermal decomposition reaction of metal oxalates have been widely investigated [1-9].The influence of the atmosphere on the course of the thermal decomposition of oxalate was exothermic in character where as the majority of such decomposition in an inert atmosphere was endothermic[10-16.Doremicux and Boule [17] have also determined the decomposition characteristics of manganese, Iron,Cobalt,Zinc and Copper oxalates in the air and nitrogen atmospheres and reported a shift to lower temperature when oxygen is present for iron, manganese and cobalt oxalates but not for zinc and copper oxalates. The thermal, spectral and magnetic studies of compound of copper and zinc carboxylates have also been studied [18-21].

We have been using the electrical conductivity techniques in the study of solid state decomposition reactions of different metal (II) carboxylates [22-24] and this chapter is a continuation of our earlier work. In this chapter we will report the thermal decomposition of copper (II) oxalate monohydrate and Zinc (II) oxalate dihydrate have been studied using two-probe d.c.electrical conductivity measurements to study the progress of reaction. This study has been supplemented with TGA, DTG and DTA, X-ray diffraction and Infrared spectroscopy.

## EXPERIMENTAL

The procedure for synthesis of copper (II) oxalate monohydrate ( $\text{CuC}_2\text{O}_4 \cdot \text{H}_2\text{O}$ ) and zinc (II) oxalate dihydrate ( $\text{ZnC}_2\text{O}_4 \cdot 2\text{H}_2\text{O}$ ) by usual way. The experimental used for the determination of various physical properties viz. Infrared spectrum ,magnetic moment ,thermal analyses (TGA,DTG and DTA ),X-ray powder diffraction and direct current electrical conductivity.

## RESULT AND DISCUSSION

### Characterization of $\text{CuC}_2\text{O}_4 \cdot \text{H}_2\text{O}$ and $\text{ZnC}_2\text{O}_4 \cdot 2\text{H}_2\text{O}$

The results of the chemical analysis (Table I ) show that there is a good agreement between found and calculated values of metal ,Carbon and Hydrogen content for the

proposed formula  $\text{CuC}_2\text{O}_4 \cdot \text{H}_2\text{O}$  and  $\text{ZnC}_2\text{O}_4 \cdot 2\text{H}_2\text{O}$ . The infrared spectrum (Fig.1) showed frequencies corresponding to the carboxylate group, Hydroxyl group, metal-oxygen etc. are given in Table II. It is known that the coordination of oxalate anion leads to the band shift of symmetric and antisymmetric C=O stretching frequencies [25-26]. The symmetric stretching frequency will decrease with the covalent bond formation between the cation and oxygen. The difference between the two stretching peaks will increase with the increased covalent character and exceed  $225 \text{ cm}^{-1}$ . The bidentate linkage to be more favorable of the oxalate group with the metal was confirmed on the basis of the difference between the antisymmetric and symmetric (C=O) stretching frequencies (Fig.1).

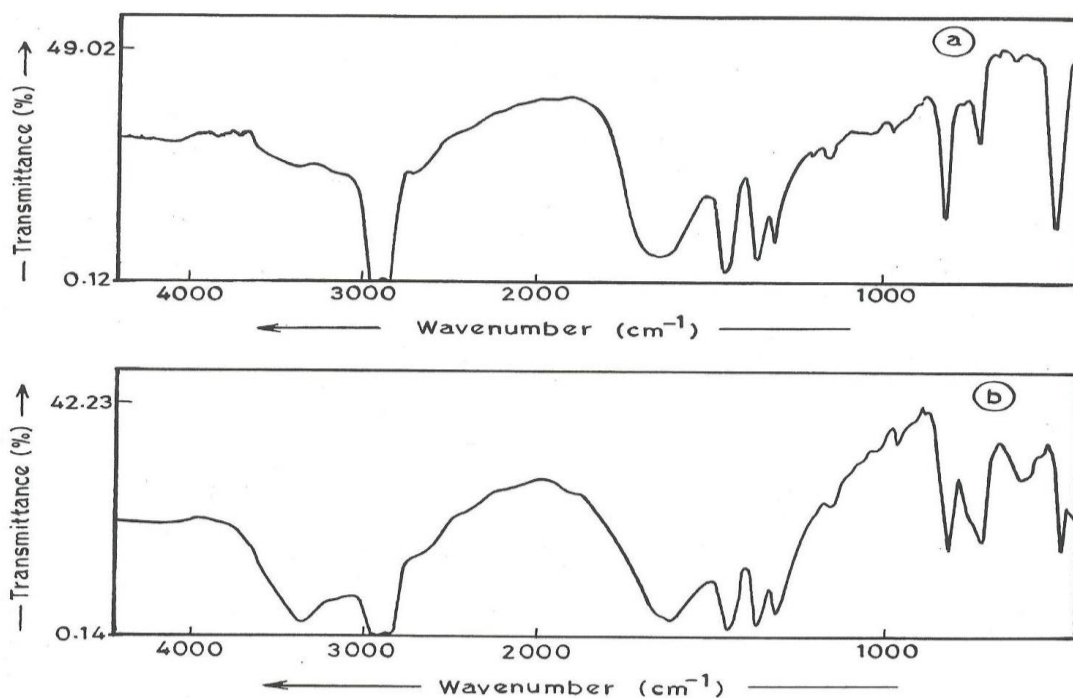


Fig. 1. Infrared spectra of (a) copper (II) oxalate monohydrate ( $\text{CuC}_2\text{O}_4 \cdot \text{H}_2\text{O}$ ) and (b) zinc (II) oxalate dihydrate ( $\text{ZnC}_2\text{O}_4 \cdot 2\text{H}_2\text{O}$ ).

**Table I: Analytical data of copper (II) Oxalate monohydrate ( $\text{CuC}_2\text{O}_4 \cdot \text{H}_2\text{O}$ ) and Zinc (II) oxalate dihydrated ( $\text{ZnC}_2\text{O}_4 \cdot 2\text{H}_2\text{O}$ )**

Compound	Formula	Formula Weight	Elemental Analysis in wt. %						Magnetic moment ( $\mu$ ) B.M.
			C		H		Metal		
			Calc.	Found	Calc.	Found	Calc.	Found	
Copper (II) Oxalate monohydrated (Colour – Light bluish green )	$\text{CuC}_2\text{O}_4 \cdot \text{H}_2\text{O}$	169.54	14.16	15.01	1.18	1.24	37.47	38.00	1.96
Zinc (II) Oxalate dihydrate (Colour- White)	$\text{ZnC}_2\text{O}_4 \cdot 2\text{H}_2\text{O}$	189.37	12.67	12.83	2.11	2.22	34.52	35.08	Diamagnetic

**Table II: X-ray diffraction data of  $\text{CuC}_2\text{O}_4 \cdot \text{H}_2\text{O}$  and  $\text{ZnC}_2\text{O}_4 \cdot 2\text{H}_2\text{O}$** 

Observed d-spacing Values ( $\text{Å}^\circ$ ) $\text{CuC}_2\text{O}_4 \cdot \text{H}_2\text{O}$	Observed d-spacing values ( $\text{Å}^\circ$ ) $\text{ZnC}_2\text{O}_4 \cdot 2\text{H}_2\text{O}$
4.66(8)	4.67 (100)
3.86(100)	3.86(39)
2.80(16)	3.56(22)
2.49(30)	2.96(72)
	2.67(23)
	2.63 (48)
2.45(25)	2.59(28)
2.36(19)	2.54(46)
2.17(12)	2.33(20)
1.95(24)	2.19(40)
1.78(36)	2.12(23)
	2.08(13)
	2.00(41)
1.71(22)	1.97(17)
1.62(26)	1.90(32)
1.56(17)	1.85(28)
1.52(14)	1.77(20)
1.48(47)	1.68(17)
	1.64(16)
1.32(10)	1.61(23)
1.31(12)	1.57(18)
1.29(8)	1.52(32)
1.23(11)	1.50(8)
1.17(8)	1.46(16)
	1.35(21)
	1.29(18)
	1.21(15)
	1.10(26)

a. The figures given in the parentheses are intensities relative to the line width intensities (100).

The infrared spectrum of  $\text{CuC}_2\text{O}_4 \cdot \text{H}_2\text{O}$  and  $\text{ZnC}_2\text{O}_4 \cdot 2\text{H}_2\text{O}$  showed a broad band at  $3440 \text{ cm}^{-1}$  ( $3450 \text{ cm}^{-1}$ ) due to (-OH) stretching, a broad band at  $1660 \text{ cm}^{-1}$  and  $1680 \text{ cm}^{-1}$  due to  $\nu_{\text{asy}}(\text{C}=\text{O})$  and band at  $1455 \text{ cm}^{-1}$  and  $1376 \text{ cm}^{-1}$  due to  $\nu_{\text{sy}}(\text{C}-\text{O})$  of coordinated oxalate group [25]. An increase in oxalate resonance leads to single-bond character in the carboxyl group, which is observed as a lowering of the frequency of the compounds, indicate a six-coordinate environment for the metal ions [26].

In all these complexes the metal has polymeric octahedral co-ordination [27]. The presence of water of crystallization was confirmed on the basis of the thermal analysis curve. The compound  $\text{CuC}_2\text{O}_4 \cdot \text{H}_2\text{O}$  has magnetic moment of 1.96 B.M.; While  $\text{ZnC}_2\text{O}_4 \cdot 2\text{H}_2\text{O}$  has zero magnetic moment, which indicates that the compound have the distorted octahedral stereochemistry.

### **Thermal decomposition processes of $\text{CuC}_2\text{O}_4 \cdot \text{H}_2\text{O}$ and $\text{ZnC}_2\text{O}_4 \cdot 2\text{H}_2\text{O}$ :**

#### **Static air atmosphere:**

#### **Copper (II) Oxalate Monohydrated:**

The TGA, DTG and DTA curves for  $\text{CuC}_2\text{O}_4 \cdot \text{H}_2\text{O}$  are shown in Fig.2 (d). The dehydration of  $\text{CuC}_2\text{O}_4 \cdot \text{H}_2\text{O}$  was indicated by the presence of one broad endothermic peak in the DTA and a peak at same temperature on DTG curve. The TGA curve showed a clear dehydration step corresponding to the loss of one water molecules from  $105\text{-}200 \text{ }^\circ\text{C}$ . (Calc., 10.62 % ; Found 11.01%). The oxidative decomposition step was represented by a strong and broad peak on the  $\delta$  and DTG curve at  $315 \text{ }^\circ\text{C}$  (Fig. 2 (a) ) The curve exhibited continuous weight loss until it crystallized to  $\text{CuO}$ . (Calc., 47.51 % ; Found 48.00 %) Above  $330 \text{ }^\circ\text{C}$  the lifting up weight loss was observed on TGA curve. This may be due to the non-stoichiometry (or Defects) present in the final product.

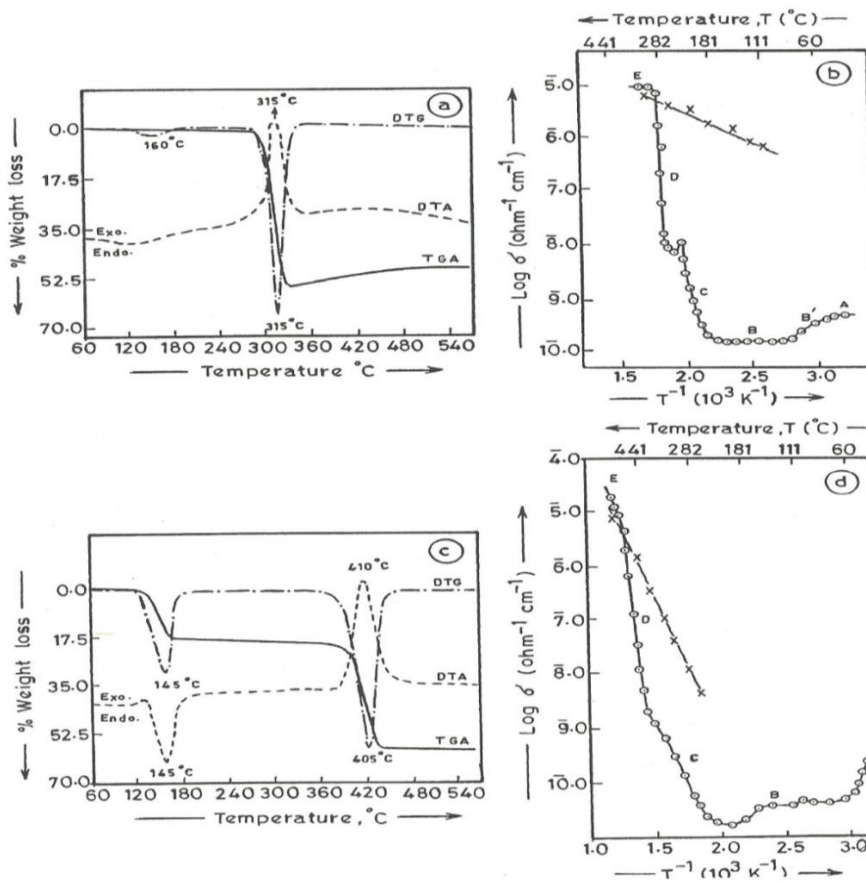


Fig. 2. Thermal decomposition in a static air atmosphere.  
 (a) TGA, DTG and DTA curves for  $\text{CuC}_2\text{O}_4 \cdot \text{H}_2\text{O}$ ;  
 (b) Plot of  $\log \delta$  vs.  $T^{-1}$  for  $\text{CuC}_2\text{O}_4 \cdot \text{H}_2\text{O}$ ;  
 (c) TGA, DTG and DTA curves for  $\text{ZnC}_2\text{O}_4 \cdot 2\text{H}_2\text{O}$ ;  
 (d) Plot of  $\log \delta$  vs.  $T^{-1}$  for  $\text{ZnC}_2\text{O}_4 \cdot 2\text{H}_2\text{O}$ ;  
 $\circ$  during decomposition; X, cooling cycle.

The plot of  $\log \delta$  vs.  $T^{-1}$  in fig. 2(b) showed a region B at 83-182  $^{\circ}\text{C}$  for dehydration step. The isothermally heated sample of  $\text{CuC}_2\text{O}_4 \cdot \text{H}_2\text{O}$  under static air, at 170 $^{\circ}\text{C}$  showed no OH band in infrared spectrum. An additional band appeared at 798 $\text{cm}^{-1}$  while other oxalate group band appeared for the parent compound also showed a blue shift. The X-ray diffraction pattern Fig.3(b) showed polycrystallinity of the sample with decrease in interplanar spacing (Table III) as compared to the parent compound shown in Fig.3(a); Table II. The elemental analysis were in good agreement with the formula  $\text{CuC}_2\text{O}_4 \cdot \text{H}_2\text{O}$ . Region b of the plot of  $\log \delta$  vs.  $T^{-1}$  shown in oxalate. Such a change is probably associated with a change from the octahedral geometry of copper (II) to tetrahedral form.

**Table III: X-ray diffraction data for anhydrous  $\text{Cu}_2\text{O}_4$  and  $\text{Zn}_2\text{O}_4$  obtained from  $\text{Cu}_2\text{O}_4 \cdot \text{H}_2\text{O}$  and  $\text{Zn}_2\text{O}_4 \cdot 2\text{H}_2\text{O}$  by heating in an atmosphere of nitrogen at 170 °C and 200 °C respectively<sup>a</sup>**

Observed d-spacing for $\text{Cu}_2\text{O}_4$ (Å <sup>o</sup> )	Observed d-spacing for $\text{Zn}_2\text{O}_4$ (Å <sup>o</sup> )
4.92(14)	4.79(10)
4.43(12)	3.78(100)
4.04(100)	3.60(18)
3.70(14)	2.81(32)
2.79(14)	2.66(28)
2.22(23)	2.48(20)
2.10(31)	2.17(10)
1.97(18)	1.99(19)
1.80(14)	1.77(21)
1.65(27)	1.60(25)
1.58(8)	1.47(30)
1.43(9)	

<sup>a</sup> The figures given in the parenthesis are intensities relative to the line width intensity (100)

After the dehydration step; the value of  $\delta$  increased steadily from 182 to 240°C (Region C). The infrared spectrum of the isothermally heated sample of  $\text{Cu}_2\text{O}_4 \cdot \text{H}_2\text{O}$  at 215°C showed a decrease in the intensities of co-ordinated carboxylate band; in addition bands at 615 (S)  $\text{cm}^{-1}$  and 410 (m)  $\text{cm}^{-1}$  occurred for metal-oxygen stretching frequencies due to the presence of cuprous oxide [28]. The x-ray diffraction of this isothermally heated sample (Table IV) was generally broad (Fig.3(c)). The pattern corresponded to anhydrous  $\text{Cu}_2\text{O}_4$  and  $\text{Cu}_2\text{O}$  [29-30]. A sharp increase in the values of  $\delta$  was observed within the temperature range 250-300 °C (Region D). For the sample heated isothermally at 280 °C, the infrared spectrum a weak band corresponding to the oxalate group, but a strong band was observed at 400  $\text{cm}^{-1}$ . The x-ray diffraction pattern of this isothermally heated sample was complex, probably corresponding to mixture of  $\text{Cu}_2\text{O}$ ,  $\text{Cu}_2\text{O}_4$  and  $\text{CuO}$ . Thus the step increase in conductivity observed in Region D was due to the transformation of  $\text{Cu}_2\text{O}_4$  to  $\text{CuO}$ , possibly via the semiconducting range of region E in Fig.2(b), the value of  $\delta$  remained almost constant. The sample obtained by heating isothermally in static air at 325°C showed a black oxide. The x-ray diffraction pattern observed for this region indicated a predominance of  $\text{CuO}$  (Table V) [31]. No line which could be assigned to metallic copper was detected in our work. The Sample thus obtained at 325 °C shows a change in  $\delta$  as the temperature is changed.

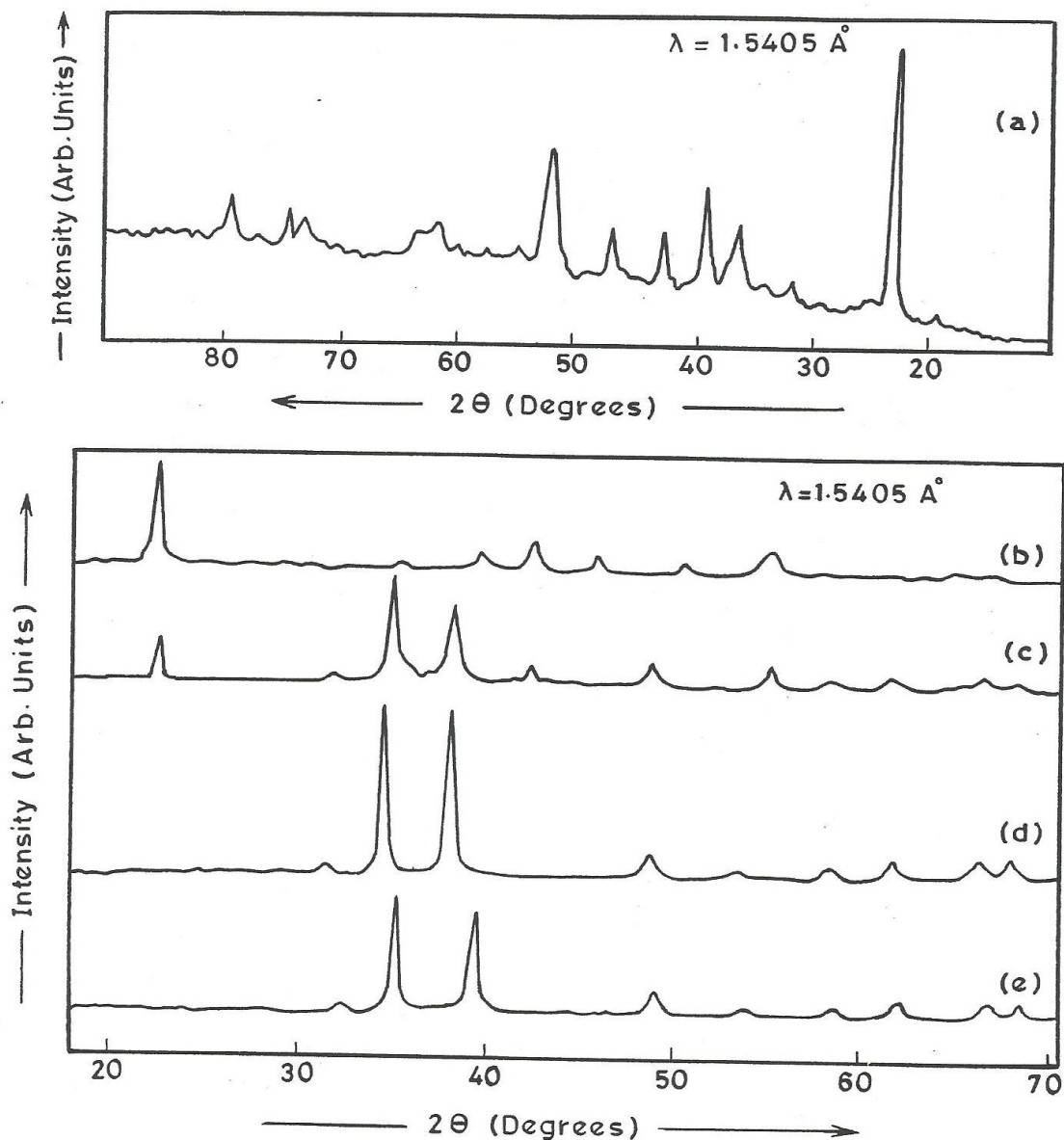


Fig. 3. X-ray diffraction patterns of copper (II) oxalate monohydrate ( $\text{CuC}_2\text{O}_4 \cdot \text{H}_2\text{O}$ ) and its decomposed products at various temperatures. (a)  $\text{CuC}_2\text{O}_4 \cdot \text{H}_2\text{O}$ ; (b)  $170^\circ\text{C}$ ; (c)  $215^\circ\text{C}$ ; (d)  $325^\circ\text{C}$ ; (e)  $320^\circ\text{C}$  (nitrogen atmosphere).



**Table IV: X-ray diffraction data for  $\text{CuC}_2\text{O}_4$  and  $\text{Cu}_2\text{O}$  obtained from  $\text{CuC}_2\text{O}_4 \cdot \text{H}_2\text{O}$  by heating in atmosphere of static air at  $215^\circ\text{C}$ <sup>a</sup>**

Observed d-spacing( $\text{Å}$ ) <sup>o</sup>	$\text{Cu}_2\text{O}$ d-spacing( $\text{Å}$ ) <sup>o</sup>
3.80(72)	
3.56(6)	
3.02(11)	3.02(9)
2.85(21)	
2.63(12)	
2.47(100)	2.46(100)
2.35(9)	
2.20(6)	
2.16(45)	2.14(37)
1.93(5)	
1.66(20)	
1.54(35)	1.51(27)
1.43(8)	
1.31(28)	1.29(17)
1.20(10)	1.23(4)
	1.07(2)
0.96(8)	0.98(4)
	0.95(3)
	0.87(3)
	0.82(3)

<sup>a</sup> The figures given in the parenthesis are intenssities relative to the linewidth intensity (100)<sup>b</sup> Ref.No.29.

**Table V: X-ray diffraction data for  $\text{CuO}$  obtained from  $\text{CuC}_2\text{O}_4 \cdot \text{H}_2\text{O}$  by heating in atmosphere of static air at  $325^\circ\text{C}$ <sup>a</sup>**

Observed d-spacing( $\text{Å}$ ) <sup>o</sup>	$\text{CuO}$ d-spacing( $\text{Å}$ ) <sup>o</sup>
2.75(19)	2.75(12)
2.55(40)	2.53(49)
2.53(100)	2.52(100)
2.33(91)	2.32(96)
2.28(42)	2.31(30)
1.88(30)	1.87(25)
1.73(15)	1.71(08)
1.57(19)	1.58(14)
1.50(23)	1.50(20)
1.41(25)	1.42(15)
1.38(24)	1.37(19)
1.29(10)	1.30(07)
	1.17(05)
	1.09(06)
	0.98(04)

<sup>a</sup> The figures given in the parentheses are intensities relative to the line width intensity (100)<sup>b</sup> Ref.No.31.

## ZnC<sub>2</sub>O<sub>4</sub>.2H<sub>2</sub>O

Figure 2 ( C ) showed the simultaneous TGA, DTG and DTA curves of ZnC<sub>2</sub>O<sub>4</sub>.2H<sub>2</sub>O. The DTA curve showed one endothermic peak at 145 °C and a peak in DTG was at 140 °C . The TGA curve at 110 °C showed a loss of 19.41 % and plateau up to 360 °C , indicating the elimination of two water molecules of crystallization ( Calc. loss = 19.01 % ) .Thereafter , the decomposition was very rapid . The TGA curve showed a loss of 47.25 % of 375-425 °C corresponding to the formation n of ZnO (cal. Loss= 46.94 % ) .This stage was supported by the presence of an exothermic peak at 405 °C on the DTA curve and peak at same temperature on DTG curve .

The temperature variation of the electrical conductivity  $\delta$  in Fig. 2 (d) showed a region B at 70-250 °C corresponding to the dehydration step. The ZnC<sub>2</sub>O<sub>4</sub>.2H<sub>2</sub>O sample , heated isothermally under static air at 200 °C , showed no H-OH band in infrared spectrum and the x-ray diffraction pattern (Fig.4(b) ) was less crystalline (Table III) than the parent compound (see Fig. 4 (a) ; Table II ) . The plot of  $\log \delta$  vs.  $T^{-1}$  (Fig. 2 (d)) showed a steady increase in values of  $\delta$  in the temperature range 250-410 °C (Region C ) . A sample heated isothermally in this region showed the infrared bands attributable to Zn –O stretching frequencies because more intense and those due to co-ordinated carboxyl ate decrease in intensity. The X-ray diffraction pattern (Fig 4 (c) ) showed a generally sharp lines , indicating that the the sample was predominantly crystalline. The pattern fits with the data for anhydrous Zinc Oxalate and Zinc Oxide (Table VI) [32].

**Table VI: X-ray diffraction data for ZnC<sub>2</sub>O<sub>4</sub> and ZnO obtained from ZnC<sub>2</sub>O<sub>4</sub>.2H<sub>2</sub>O by heating in atmosphere of static air at 480 °C<sup>a</sup>**

Observed d-spacing(A <sup>o</sup> )	ZnO d-spacing <sup>b</sup> (A <sup>o</sup> )
2.83(66)	2.82(71)
2.63(51)	2.60(56)
2.46(100)	2.48(100)
1.92(18)	1.91(29)
1.63(38)	1.63(40)
1.48(27)	1.48(35)
1.41(8)	1.41(6)
1.38(25)	1.38(28)
1.35(13)	1.36(14)
	1.30(3)
	1.24(5)
	1.18(3)
1.10(8)	1.09(10)
	1.06(4)
1.02(11)	1.04(10)
	1.01(5)
	0.98(7)
0.89(18)	0.91(12)
	0.88(6)
	0.84(6)

<sup>a</sup> The figures given in the parentheses are intensities relative to the line width intensity (100)  
<sup>b</sup> Ref.No.32.

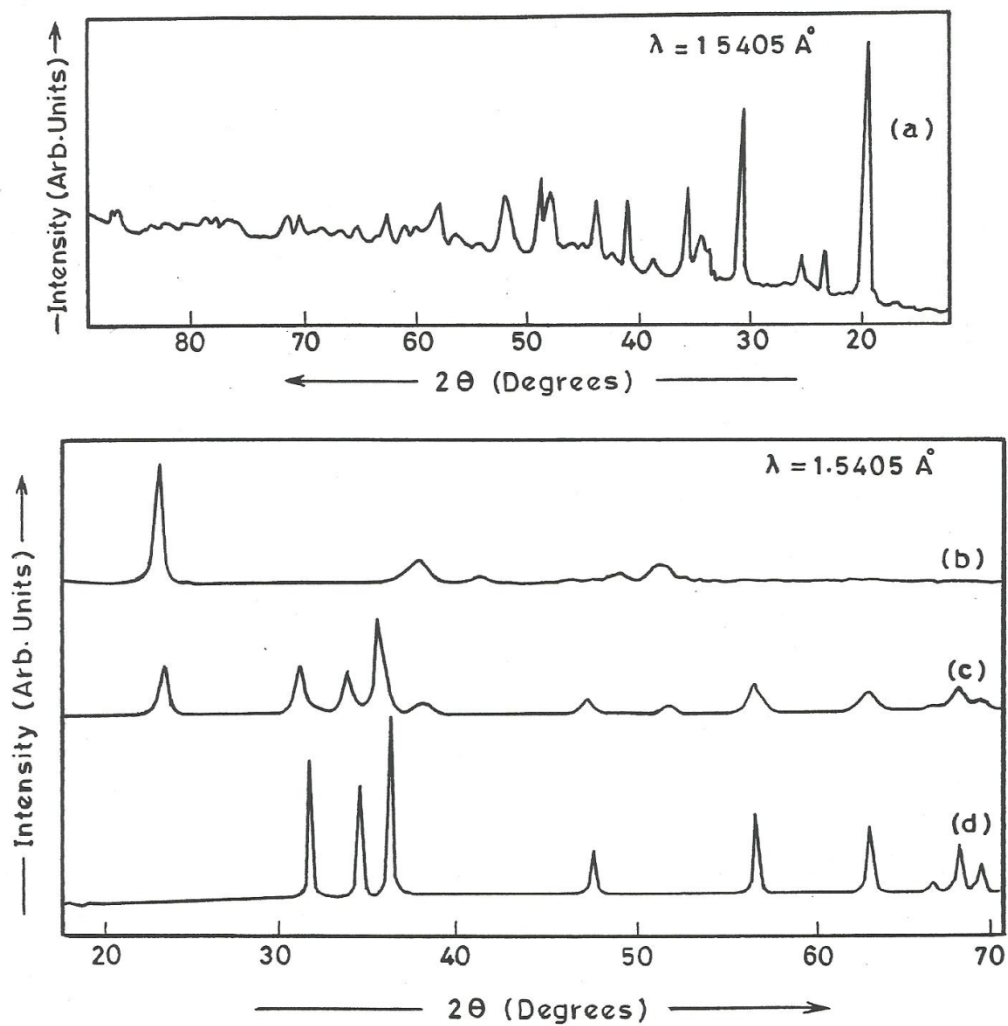


Fig. 4. X-ray diffraction patterns of zinc (II) oxalate dihydrate ( $\text{ZnC}_2\text{O}_4 \cdot 2\text{H}_2\text{O}$ ) and its decomposed products at various temperatures. (a)  $\text{ZnC}_2\text{O}_4 \cdot 2\text{H}_2\text{O}$ ; (b)  $200^\circ\text{C}$ ; (c)  $480^\circ\text{C}$ ; (d)  $420^\circ\text{C}$  (nitrogen atmosphere).

**Table VII: X-ray diffraction data for Cu<sub>2</sub>O and ZnO obtained from CuC<sub>2</sub>O<sub>4</sub>.H<sub>2</sub>O and ZnC<sub>2</sub>O<sub>4</sub>.2H<sub>2</sub>O by heating in an atmosphere of nitrogen at 320 °C and 420 °C respectively<sup>a</sup>**

Observed d-spacing for Cu <sub>2</sub> O (Å <sup>o</sup> )	Observed d-spacing for ZnO(A <sup>o</sup> )
2.98(16)	2.84(69)
2.47(100)	2.59(55)
2.16(48)	2.46(100)
1.50(21)	1.93(21)
1.32(22)	1.62(37)
1.23(10)	1.47(27)
1.05(6)	1.40(12)
0.97(11)	1.37(26)
0.90(8)	1.35(13)
	1.08(15)
	0.99(20)
	0.90(22)

<sup>a</sup> The figures given in the parentheses are intensities relative to the line width intensity (100)

A step increase in  $\delta$  was observed at 420 °C (Region D between 420°C and 480 °C, Fig 2 (d)). The infrared spectrum and X-ray diffraction pattern (Fig. 4(d)) for the sample decomposed isothermally at 480 °C showed mainly ZnO (Table VII). The sample was white and had an electrical conductivity value of about  $10^{-3} \text{ ohm}^{-1} \text{ cm}^{-1}$  [33]. The sample thus obtained at 480 °C shows a variation in  $\delta$  with temperature. This behaviour is characteristics of the non – stoichiometry present in ZnO [34-35].

Thus the conventional thermal analysis (TGA, DTG and DTA) supplemented with electrical conductivity, infrared spectrum, X-ray diffraction patterns and elemental analyses gave a detailed analysis of the thermal decomposition of CuC<sub>2</sub>O<sub>4</sub>.H<sub>2</sub>O and ZnC<sub>2</sub>O<sub>4</sub>.2H<sub>2</sub>O. It is well known that the solid state thermal decomposition of metal oxalate are influenced by the atmosphere [10-17]; it was decided to undertake similar measurements in other controlled atmospheres.

### Dynamic Nitrogen Atmosphere

#### CuC<sub>2</sub>O<sub>4</sub>.H<sub>2</sub>O:

The TGA curve for CuC<sub>2</sub>O<sub>4</sub>.H<sub>2</sub>O in Fig.5(a) showed a clear dehydration step corresponding to the loss of one water molecules from 90 to 210 °C and this stage is supported by the presence of an endothermic peak at 170 °C on the DTA curve and a peak at same temperature on DTG curve . The decomposition of the oxalate (CuC<sub>2</sub>O<sub>4</sub> ) was indicated by an endothermic peak in the DTA curve at 320 °C and in the DTG curve at 315 °C .This weight loss was found to be in good agreement with the formation of Cu<sub>2</sub>O (Calc.,52.79 % ;Found 53.08 %) as the final product . The plot of  $\log \delta$  vs.  $T^{-1}$  (Fig. (b) ) showed that  $\delta$  was initially constant , but then decreased steadily and remained constant up to 225 °C (Region B ) . The infrared spectrum, elemental analysis and x-ray diffraction pattern (Similar

to Fig.3 (b) ) confirmed the formation of anhydrous copper oxalate in this region . After the dehydration step, the value of  $\delta$  increased steadily within the temperature range 225-285 °C (Region C) and then a step increase in  $\delta$  at 285-320 °C (Region D). The x-ray diffraction pattern (Fig.3(c)) and infrared spectrum for a sample heated isothermally in region C showed a mixture of  $\text{CuC}_2\text{O}_4$  and  $\text{Cu}_2\text{O}$ . The x-ray diffraction pattern (Fig .3(c)) for a sample from the dry nitrogen atmosphere obtained at 320 °C (Region D) showed a variation in  $\delta$  with changing in temperature. This behavior is characteristic of  $\text{Cu}_2\text{O}$  [30]. The sample was red in color .Thus the x-ray diffraction patterns and conductivity measurements suggested that the product obtained by thermal decomposition of  $\text{CuC}_2\text{O}_4 \cdot \text{H}_2\text{O}$  in a dry nitrogen atmosphere is pure  $\text{Cu}_2\text{O}$  ,and that the concentration of copper metal ,if present at all ,is beyond the detection limit of these techniques. [35-38]

### **$\text{ZnC}_2\text{O}_4 \cdot 2\text{H}_2\text{O}$**

The TGA, DTG and DTA curves of  $\text{ZnC}_2\text{O}_4 \cdot 2\text{H}_2\text{O}$  are shown in Fig.5(C) .Dehydration of  $\text{ZnC}_2\text{O}_4 \cdot 2\text{H}_2\text{O}$  was indicated by endothermic peak in the DTA and a peak in DTG curves at 150 °C The TGA curve showed a weight loss with the range 80-170 °C ,with a plateau up to 360 °C corresponding to the loss of two water molecules . The decomposition of the oxalate ( $\text{ZnC}_2\text{O}_4$ ) was indicated by an endothermic peak in the DTA curves at 415 °C .The TGA curves showed a continuous weight loss 360 -420 °C . This weight loss was found to be in good agreement with the formation of ZnO.

Region B in the plot of  $\log$  vs.  $T^{-1}$  (fig. 5 (d) ) corresponding to the dehydration of  $\text{ZnC}_2\text{O}_4 \cdot 2\text{H}_2\text{O}$  . There was step increase in  $\delta$  at 320 °C followed by another step increase at 417 °C (see Region C and D , in Fig. 5 (d) ). These two temperature ranges, 320-410 °C and 415- 445 °C, can be tentatively assigned to the formation of zinc oxide together with some  $\text{ZnC}_2\text{O}_4$  and ZnO, respectively .The X- ray diffraction and infrared spectrum confirmed the formation of these phases. Thus the x- Ray diffraction and conductivity measurement suggested that the product obtained by thermal decomposition of  $\text{ZnC}_2\text{O}_4 \cdot 2\text{H}_2\text{O}$  in a nitrogen atmosphere is pure ZnO.

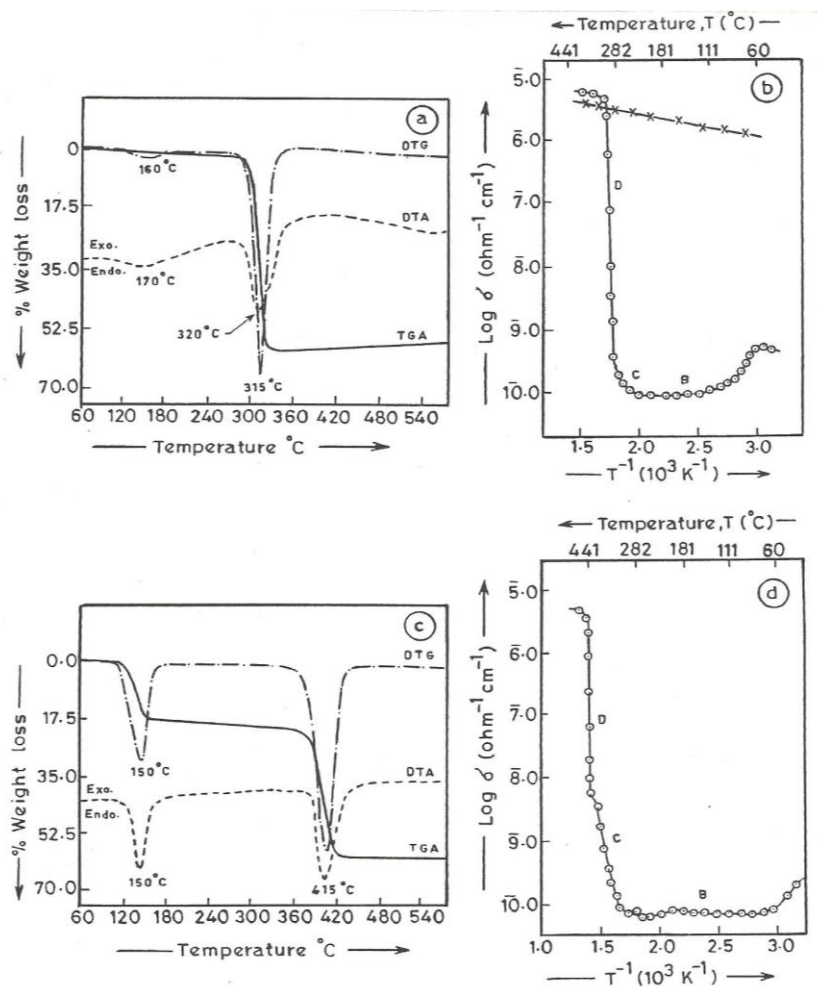


Fig. 5 Thermal decomposition in a dynamic nitrogen atmosphere : (a) TGA, DTG and DTA curves for  $\text{CuC}_2\text{O}_4 \cdot \text{H}_2\text{O}$ ; (b) Plot of  $\log \delta$  vs.  $T^{-1}$  for  $\text{CuC}_2\text{O}_4 \cdot \text{H}_2\text{O}$  :  $\odot$ , during decomposition;  $\times$ , cooling cycle; (c) TGA, DTG and DTA curves for  $\text{ZnC}_2\text{O}_4 \cdot 2\text{H}_2\text{O}$ ; (d) Plot of  $\log \delta$  vs.  $T^{-1}$  for  $\text{ZnC}_2\text{O}_4 \cdot 2\text{H}_2\text{O}$ .

## Dynamic air atmosphere

### $\text{CuC}_2\text{O}_4 \cdot \text{H}_2\text{O}$

In Fig. 6 (a), for  $\text{CuC}_2\text{O}_4 \cdot \text{H}_2\text{O}$ , the DTA and DTG curves showed a peak at  $160^\circ\text{C}$  for dehydration step and TGA curve also produced a weight loss beginning at  $100\text{--}190^\circ\text{C}$  corresponded to the removal of the water molecule contained in this oxalate. The broad exothermic peak corresponding to oxidative decomposition was shown on the DTA curves  $310^\circ\text{C}$  and peak at curve shown on the DTG curve.

The TGA curve showed a continuous weight loss in this region, where the material finally crystallized to  $\text{CuO}$ . Supplementing the  $\log \delta$  vs.  $T^{-1}$  measurements (in Fig. 6 (b)) revealed the dehydration and the nature of the decomposition is similar to that shown in

Fig. 2 (b) . The isothermal decomposition under a dynamic air atmosphere for  $\text{CuC}_2\text{O}_4 \cdot \text{H}_2\text{O}$  at various temperature region showed that the product obtained were similar to those from isothermally decomposition  $\text{CuC}_2\text{O}_4 \cdot \text{H}_2\text{O}$  under a static air atmosphere.

### $\text{ZnC}_2\text{O}_4 \cdot 2\text{H}_2\text{O}$

The TGA curve showed a weight loss between 85 and 155 ° C (Fig. 6 (C) ) . The DTA curve showed an endothermic peak at 135 ° C and there was also a peak in the DTG curve at the same temperature, corresponding to the dehydration of  $\text{ZnC}_2\text{O}_4 \cdot 2\text{H}_2\text{O}$  and an exothermic peak at 405 ° C corresponding to oxidative decomposition. The TGA showed a continuous weight loss from 380 ° C until it crystallized to mainly ZnO

The plot of  $\log \delta$  vs.  $T^{-1}$  in Fig. 6 (d) was quite similar to Fig. 5 (d) . The infrared spectrum and X-ray diffraction pattern for the sample decomposed isothermally at Region B, C and d were respectively anhydrous  $\text{ZnC}_2\text{O}_4$  a mixture of  $\text{ZnC}_2\text{O}_4$  and ZnO and pure ZnO in this atmosphere. The prescribed intermediates obtained in each temperature region under all three atmospheres are shown in Tables VIII and IX.

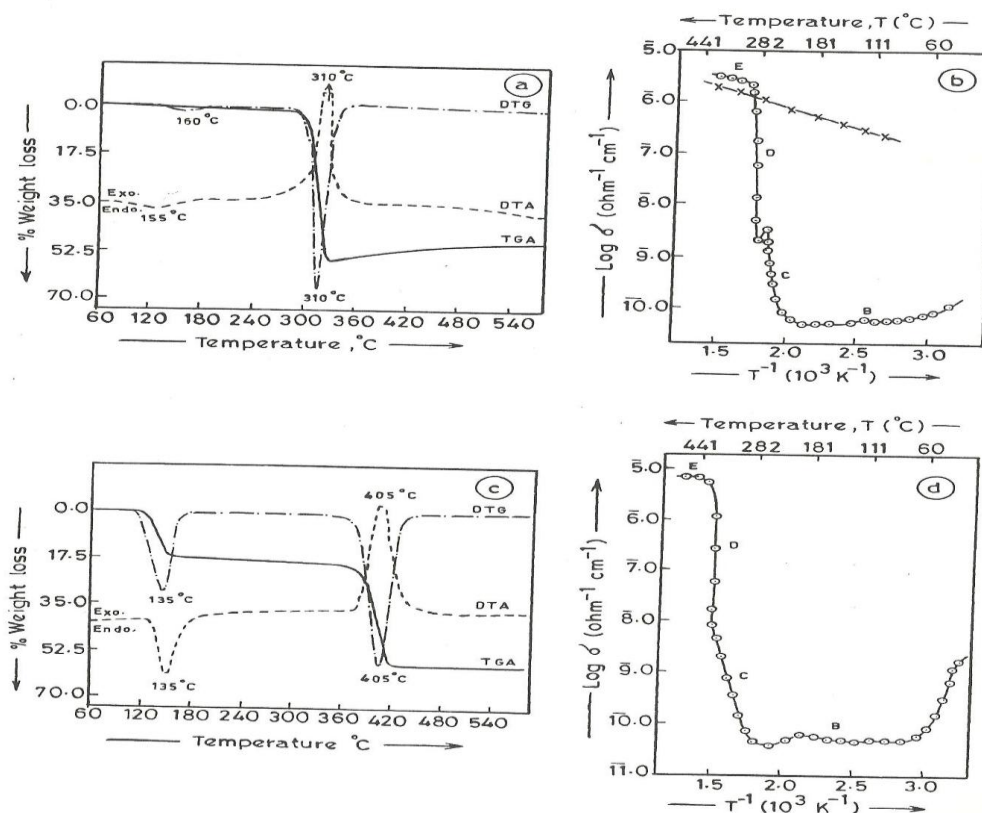


Fig. 6 Thermal decomposition in a dynamic air atmosphere.  
 (a) TGA, DTG and DTA curves for  $\text{CuC}_2\text{O}_4 \cdot \text{H}_2\text{O}$ ;  
 (b) Plot of  $\log \delta$  vs.  $T^{-1}$  for  $\text{CuC}_2\text{O}_4 \cdot \text{H}_2\text{O}$ ;  
 (c) TGA, DTG and DTA curves for  $\text{ZnC}_2\text{O}_4 \cdot 2\text{H}_2\text{O}$ ;  
 (d) Plot of  $\log \delta$  vs.  $T^{-1}$  for  $\text{ZnC}_2\text{O}_4 \cdot 2\text{H}_2\text{O}$ .

**Table VIII: Predicted intermediates and final product obtained from  $\text{CuC}_2\text{O}_4 \cdot \text{H}_2\text{O}$  under different atmospheres, measured via d.c. electrical conductivity.**

Atmosphere	Region	Temperature range °C	Predicted intermediates and final product
Static air	A	25-83	$\text{CuC}_2\text{O}_4 \cdot \text{H}_2\text{O}$
	B	83-182	$\text{CuC}_2\text{O}_4$
	C	182-240	$\text{CuC}_2\text{O}_4 + \text{Cu}_2\text{O}$
	D	240-325	$\text{CuC}_2\text{O}_4 + \text{Cu}_2\text{O} + \text{CuO}$
	E	Above 325	$\text{CuO}$
Dynamic Nitrogen	A	25-50	$\text{CuC}_2\text{O}_4 \cdot \text{H}_2\text{O}$
	B	50-225	$\text{CuC}_2\text{O}_4$
	C	225-285	$\text{CuC}_2\text{O}_4 + \text{Cu}_2\text{O}$
	D	285-320	$\text{Cu}_2\text{O}$
Dynamic air	A	25-60	$\text{CuC}_2\text{O}_4 \cdot \text{H}_2\text{O}$
	B	60-200	$\text{CuC}_2\text{O}_4$
	C	200-260	$\text{CuC}_2\text{O}_4 + \text{Cu}_2\text{O}$
	D	260-310	$\text{CuC}_2\text{O}_4 + \text{Cu}_2\text{O} + \text{CuO}$
	E	Above 310	$\text{CuO}$

**Table IX: Predicted intermediates and final product obtained from  $\text{ZnC}_2\text{O}_4 \cdot 2\text{H}_2\text{O}$  under different atmospheres, measured via d.c. electrical conductivity.**

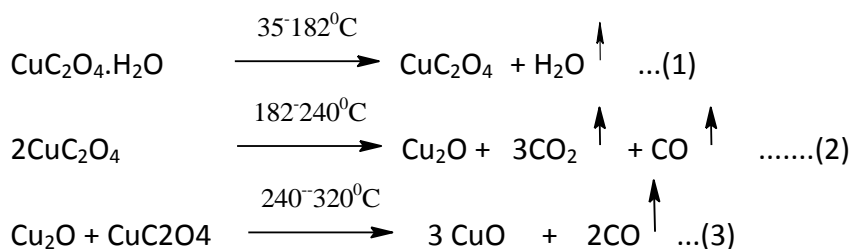
Atmosphere	Region	Temperature range °C	Predicted intermediates and final product
Static air	A	25-70	$\text{ZnC}_2\text{O}_4 \cdot 2\text{H}_2\text{O}$
	B	70-250	$\text{ZnC}_2\text{O}_4$
	C	182-240	$\text{ZnC}_2\text{O}_4 + \text{ZnO}$
	D	240-325	$\text{ZnO}$
Dynamic Nitrogen	A	25-80	$\text{ZnC}_2\text{O}_4 \cdot 2\text{H}_2\text{O}$
	B	80-320	$\text{ZnC}_2\text{O}_4$
	C	320-410	$\text{ZnC}_2\text{O}_4 + \text{ZnO}$
	D	410-445	$\text{ZnO}$
Dynamic air	A	25-75	$\text{ZnC}_2\text{O}_4 \cdot 2\text{H}_2\text{O}$
	B	75-310	$\text{ZnC}_2\text{O}_4$
	C	310-400	$\text{ZnC}_2\text{O}_4 + \text{ZnO}$
	D	400-450	$\text{ZnO}$

The gases were collected at around 410 °C on the thermal decomposition of the parent compounds ( i.e.  $\text{CuC}_2\text{O}_4 \cdot \text{H}_2\text{O}$  and  $\text{ZnC}_2\text{O}_4 \cdot 2\text{H}_2\text{O}$  ) under a dynamic nitrogen atmosphere . The qualitative gas analyses showed the presence of carbon monoxide and carbon dioxide. An increase in oxalate resonance leads to single-bond character in the carboxyl group, which is observed as a lowering of the frequency

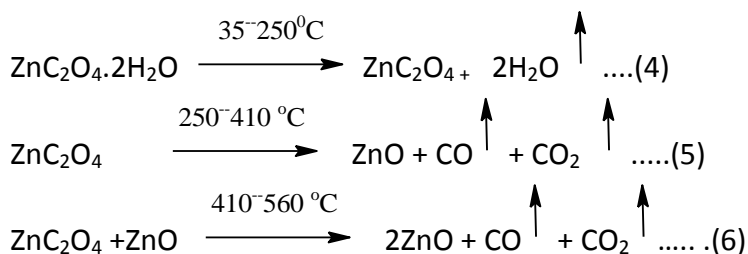
The different paths followed by the decomposition of  $\text{CuC}_2\text{O}_4 \cdot \text{H}_2\text{O}$  and  $\text{ZnC}_2\text{O}_4 \cdot 2\text{H}_2\text{O}$  in different atmospheres showed complete dehydration from conductivity measurements,



thermal analyses (TGA,DTA and DTA ) and the infrared spectrum .A transformation of  $\text{Cu}_2\text{O}_4 \cdot \text{H}_2\text{O}$  and  $\text{CuO}$  and dynamic air atmospheres. These reactions bare presented as follows:



The transformation of  $\text{Cu}_2\text{O}_4$  to  $\text{Cu}_2\text{O}$  was the final step detected in a dynamic dry nitrogen atmosphere , which  $\text{Zn}_2\text{O}_4$  transform to  $\text{ZnO}$  under static air , dynamic dry nitrogen and dynamic air atmospheres .



### CONCLUSION

The present study revealed following finding on the solid –state dehydration of  $\text{Cu}_2\text{O}_4 \cdot \text{H}_2\text{O}$  and  $\text{Zn}_2\text{O}_4 \cdot 2\text{H}_2\text{O}$  .

- (a) The dehydration of  $\text{Cu}_2\text{O}_4 \cdot \text{H}_2\text{O}$  and  $\text{Zn}_2\text{O}_4 \cdot 2\text{H}_2\text{O}$  yielding anhydrous  $\text{Cu}_2\text{O}_4$  or  $\text{Zn}_2\text{O}_4$  ,took place in all three of the atmospheres considered.
- (b) In dry nitrogen, the formation of  $\text{Cu}_2\text{O}$  from  $\text{Cu}_2\text{O}_4 \cdot \text{H}_2\text{O}$  was confirmed by using d.c. electrical conductivity measurements , in conjunction with infrared spectrum and X-ray diffraction investigations.
- (c) The final product of decomposition in static air and dynamic air was found to be  $\text{CuO}$  for  $\text{Cu}_2\text{O}_4 \cdot \text{H}_2\text{O}$  .However , the final decomposition product in all three atmospheres was found to  $\text{ZnO}$  for  $\text{Zn}_2\text{O}_4 \cdot 2\text{H}_2\text{O}$  .
- (d) The oxidative behavior of these oxalates was better understood from the study of temperature variation of d.c.electrical conductivity measurements.

### REFERENCES

- [1] D Dollimore. *Thermochim Acta* 1987; 117:331.
- [2] D Dollimore, DL Griffiths and D Nicholson. *J Chem Soc* 1963; 2617.

- [3] D Dollimore, J Dollimore and D Nicholson. J Chem Soc 1962; 960.
- [4] JV TOjko and RG Nikola. Thermochim Acta 1992; 198: 360.
- [5] R David. Bull Soc Chem Fr 1960; 717.
- [6] Ya A, Uga Z. Obshchei khem 1954; 24:1315.
- [7] K Kawagaki. J Chem Soc Japan 1951; 72:1079.
- [8] FA gooch and HL Ward. Am J Sci 1933; 27:448.
- [9] J Robin. Bull Soc Chem FR 1953:1078.
- [10] D Dollimore. J Thermo Anal 1977; 11:185.
- [11] DA Young. Determination of solids pergamon press, New York 1966; 148.
- [12] WE Garnar. Chemistry of the solid state. Butter worths Publ 1955; 232.
- [13] D Dollimore, J Dollimore and J Little. J Chem Soc 1969; 2946.
- [14] M Brown, D Dollomore and AK Gatwey. J Chem Soc 1969; 2946.
- [15] ED Macklen. J Inorg Nucl Chem 1968; 30:2689.
- [16] C Duval. Inorganic Thermogravimetric Analysis Elsevier, Amsterdam 1963.
- [17] JL Doremicux and A Bouille. CR Acad Sci Paris 1960; 250:3184.
- [18] JR Allan, BR Carson, DL Gerrard and S Hoey. Thermochim Acta 1989; 147:353.
- [19] JA Allan, GM Baillie, JG Bonner, DL Gerrard and S HOey. Thermochim Acta 1989; 143:283.
- [20] K Muraishi, K Nagase and N Tanake . Thermochim Acta 1978; 23:125.
- [21] AA Vecher, SV Dalidovich and EA Gusev. Thermochim Acta 1985; 89:383.
- [22] KS Rane, Ak Nikumbh and AJ Mukhedkar. J Mater Sci 16919810:2397.
- [23] AK Nikumbh, MM Rahman and AD Aware. Thermochim Acta 1991; 186:217.
- [24] AK Nikumbh, AE Athare and VB Raut. Thermochim Acta 1991; 186:217.
- [25] AK Nikumbh, AA Latkar and MM Phadke. Thermochim Acta 1993; 219:269.
- [26] K Nakamoto, Infrared and Ram spectra of Inorganic and Coordination compounds, Wileys, NewYork 1978.
- [27] NF Curtis. J Chem Soc A 1968:1585.
- [28] J Fujita, AE Martell and K Nakamoto. J Chem Phys 1962; 36:324-331.
- [29] ASTM file Number 5-667.
- [30] AP Young and CM Schwartz. J Phys and Chem Solids 1969; 30:249.
- [31] ASTM File Number 5-661.
- [32] ASTM File Number 5-664.
- [33] AV Krylova, L Ya Margolis and GI Chizhikova. Kinetika katali 1965; 6(5): 771-854.
- [34] WJ Moore. Seven Solid States: An introduction to chemistry and physics of slolides, W.A. Benjamin, Inc. Newyork 1967:145.
- [35] Jun L, Feng-Xing Z, Yan-Wei R, Yong-Qian H & Ye-Fei N 2003; 406(1-2):77-87.
- [36] Prasad R. 2003; 406(1-2):99-104.
- [37] Raje N & Reddy AVR. A review 2010; 505(1-2):53-58.
- [38] Pérez-Rodríguez JL, Duran A, Centeno MA, Martinez-Blanes JM & Robador MD 2011; 512(1-2):5-12.